Journal of Geophysical Research: Atmospheres

RESEARCH ARTICLE
10.1029/2018JD028821

Larger Sensitivity of Precipitation Extremes to Aerosol Than Greenhouse Gas Forcing in CMIP5 Models

Lei Lin[1], Zhili Wang[2,3], Yangyang Xu[4], Qiang Fu[5], and Wenjie Dong[1]

[1]School of Atmospheric Sciences and Guangdong Province Key Laboratory for Climate Change and Natural Disaster Studies, Sun Yat-sen University, Zhuhai, China, [2]State Key Laboratory of Severe Weather and Key Laboratory of Atmospheric Chemistry of CMA, Chinese Academy of Meteorological Sciences, Beijing, China, [3]Collaborative Innovation Center on Forecast and Evaluation of Meteorological Disasters, Nanjing University of Information Science and Technology, Nanjing, China, [4]Department of Atmospheric Sciences, Texas A&M University, College Station, TX, USA, [5]Department of Atmospheric Sciences, University of Washington, Seattle, WA, USA

Key Points:
- CMIP5 multimodel ensemble simulations robustly show a larger sensitivity of precipitation extremes to aerosol than GHG forcing
- This sensitivity difference is primarily associated with the fast response of precipitation extremes to various forcings
- This sensitivity difference depends on the definitions of precipitation extremes

Correspondence to:
Z. Wang,
wangzl@cma.gov.cn

Citation:
Lin, L., Wang, Z., Xu, Y., Fu, Q., & Dong, W. (2018). Larger sensitivity of precipitation extremes to aerosol than greenhouse gas forcing in CMIP5 models. *Journal of Geophysical Research: Atmospheres*, *123*. https://doi.org/10.1029/2018JD028821

Received 12 APR 2018
Accepted 25 JUL 2018
Accepted article online 3 AUG 2018

Abstract The sensitivity of precipitation extremes (PEs; i.e., the change in PE per degree of change in global mean surface temperature) to aerosol and greenhouse gas (GHG) forcings is examined using the twentieth century historical multimodel ensemble simulations from the Coupled Model Intercomparison Program phase 5 (CMIP5). We find a robustly larger sensitivity of PE to aerosols than GHGs across all available models. The aerosol/GHG-induced sensitivity ratios for globe-averaged monthly maximum consecutive 5-day precipitation (RX5day) and maximum 1-day precipitation (RX1day) in the multimodel ensemble are 1.6 and 1.4, respectively. Over land, the corresponding ratios for RX5day and RX1day are 2.3 and 1.8, respectively. In particular, the aerosol forcing leads to several times greater sensitivity than GHG forcing in West Africa, eastern China, South and Southeast Asia, northwestern South America, and Eastern Europe. The atmospheric energy balance, dynamical adjustment, and vertical structure of forcing, all contribute to the difference in the PE sensitivity to the two forcings. It is shown that the fast response primarily contributes to the greater-than-one aerosol-to-GHG ratios of the PE sensitivities, as for the mean precipitation. This is because of a stronger rainfall suppression effect induced by the GHG atmospheric forcing. We also find that the aerosol-to-GHG ratios of the PE sensitivities depend on the defined extreme precipitation indices. The aerosol-to-GHG sensitivity ratio is larger for more loosely defined PE, and it gradually converges to one for more severely defined PE. Our results further highlight the importance of considering the anthropogenic aerosol reduction in projecting the change in PE.

Plain Language Summary Precipitation extreme (PE) has wide-ranging societal impacts. Warming caused by greenhouse gas (GHG) increases primarily contributes to the increase in PE during recent decades. To mitigate the air pollution, the expected declines of anthropogenic aerosols in the 21st century would impose an additional warming on the Earth, which will aggravate the PE caused by GHGs-induced warming. The ultimate response of PE is thus related to the strength of various forcing agents, and the sensitivity of PE to various forcing agents. We show whether the difference in the PE sensitivity between GHGs and aerosols is robust across models and what mechanisms lead to the difference. A robustly larger sensitivity of PE to aerosols than GHGs across all available models is found. This sensitivity difference is primarily associated with the fast response of PE to various forcings. This study further highlights the importance of considering the anthropogenic aerosol reduction in projecting the change in PE. It has implications for policy making on climate adaptation to PE.

1. Introduction

Precipitation extremes (PEs) have wide-ranging impacts on social economy and the global ecosystem (Easterling et al., 2000; Knapp et al., 2008). However, attribution of past long-term (decadal to centennial) changes in PE to various anthropogenic factors is under intense scrutiny (Myhre et al., 2017). Previous studies have shown that the frequency and intensity of PE have increased with global warming (Hartman et al., 2013; O'Gorman, 2015). The multimodel ensemble (MME) simulations from the Coupled Model Intercomparison Program phase 5 (CMIP5) suggested that the sensitivity of PE to global warming (defined here as the change in PE per degree of change in global mean surface temperature and denoted as $\Delta PE/\Delta GMST$) was about 6%/°C (Kharin et al., 2013). Using a global high-quality land-based observational data set, Westra et al. (2013)

showed that the rate of increase in annual maximum daily precipitation with increase in GMST was between 5.9%/°C and 7.7%/°C.

While greenhouse gases (GHGs) contribute to the observed warming during the past century, anthropogenic aerosols have partly offset the GHG-induced warming (Myhre et al., 2013). To mitigate the air pollution, anthropogenic aerosol emissions would likely be cut drastically in the coming decades, as projected in the Representative Concentration Pathways (Moss et al., 2010) and more recently in the Shared Socioeconomic Pathways (Rao et al., 2016). Actually, that has occurred. As a result of emission control policies, sulfur dioxide (SO_2) emissions in China have been reduced by 75% in the recent decade (Li et al., 2017), and SO_2 emissions over Europe and North American have declined since the 1980s (Hoesly et al., 2018). The decreased aerosol emissions would weaken the aerosol net negative forcing at the top of the atmosphere and exert an additional warming effect on the future Earth's climate (Lin et al., 2018; Xu et al., 2015), which would aggravate the PE increase due to GHGs (Sillmann, Kharin, et al., 2013; Wang, Lin, et al., 2016). It is likely that the ultimate response of PE is related to the strength of various forcing agents (W/m^2; Sillmann, Pozzoli, et al., 2013), and the sensitivity of PE to various forcing agents, such as GHGs versus aerosols (Lin et al., 2016). Therefore, further understanding of the sensitivity of PE to different forcings has implications for projection of PE and policy making on climate adaptation to PE.

The recent work given by Pendergrass et al. (2015) showed that change in PE only depended on the total amount of surface warming and not on the emission scenarios in most global climate models (GCMs). Nevertheless, they have not explored the sensitivity of PE to different forcing agents. Sillmann et al. (2017) found that there was no significant difference in the PE sensitivity between GHG and solar forcings on a global scale. However, we examined the PE sensitivity to aerosol and GHG forcings using the 21st century simulations from a single GCM (Community Earth System Model version 1, CESM1; Lin et al., 2016). Our results indicated that the 21st century aerosol forcing would lead to a $\Delta PE/\Delta GMST$ that is 2–4 times of that due to the GHG forcing, which means that the sensitivity of PE significantly likely depends on the composition of forcing in emissions scenarios. Several potential explanations to the significant greater-than-one ratio between aerosol- and GHG-induced sensitivities were qualitatively discussed (Lin et al., 2016). First and foremost, the latent heat release of rainfall is the main balancing term of atmospheric radiative cooling at a global scale, and therefore, atmospheric heating caused by GHGs has a suppression effect on the rainfall increase. In contrast, the aerosol forcing has a much smaller atmospheric forcing term, and thus a smaller suppression impact on hydrologic cycle than GHGs. Second, the spatially inhomogeneous aerosol forcing can alter the rainfall partitioning between ocean and land. Third, aerosols could also impact the rainfall through perturbing cloud microphysics that would change the cloud albedo and cloud lifetime, a mechanism that is missing in the GHG-induced response.

However, important questions remain. (1) Since the sensitivity of PE to a forcing agent would likely vary for different climate models (Andrews et al., 2012), it is not clear whether the results in Lin et al. (2016) are robust or model dependent. (2) Although several plausible mechanisms for the PE sensitivity difference due to GHGs and aerosols were discussed, their importance and relative contributions were not quantified. (3) The GHG-induced response in Lin et al. (2016) was derived from the 21st century all-forcing experiment under the Representative Concentration Pathways 8.5 scenario except that aerosol emissions are fixed at the year 2005 levels, which inevitably included the effect of forcings other than long-lived GHGs, such as tropospheric and stratospheric ozone and land use.

In order to address these issues, this study explores the sensitivity of PE to aerosol and GHG forcings using the CMIP5 multimodel historical simulations. We systematically examine how the difference in the PE sensitivity between GHGs and aerosols is related to the geographic locations (e.g., land vs. ocean), vertical structure of forcing, PE definition, aerosol model treatments, and rainfall types. The current understanding of mean precipitation changes from different climate forcings has indicated that the fast response leads to the difference in the sensitivity of mean precipitation to GHGs and aerosols (e.g., Kvalevåg et al., 2013; Samset et al., 2016). It reflects the fact that precipitation amount is strongly constrained by atmospheric radiative energy (Allen & Ingram, 2002). This drives us to decompose the fast and slow PE responses to the forcings, enabling an examination of physical mechanism responsible for the different sensitivities. Section 2 describes the data and methods used in this study. Section 3 shows the PE sensitivity difference between various forcings in the MME simulations and analyzes the physical mechanisms. The discussion and summary are provided in sections 4 and 5, respectively.

Table 1
The 17 CMIP5 Models and Simulations Used in This Study

	Historical GHG	Historical AEROSOL	sstClim	sstClim4×CO_2	sstClimAerosol
BCC_CSM1.1 (2.815° × 2.815°)	✓		✓	✓	✓
CanESM2 (2.815° × 2.815°)	✓	✓	✓	✓	✓
CNRM-CM5 (1.4° × 1.4°)	✓				
CSIRO-Mk3–6-0 (1.875° × 1.875°)	✓	✓	✓	✓	✓
IPSL-CM5A-LR (3.75° × 1.875°)	✓	✓	✓	✓	✓
IPSL-CM5A-MR (2.5° × 1.25°)	✓				
MIROC5 (1.4° × 1.4°)			✓	✓	✓
MIROC-ESM (2.815° × 2.815°)	✓				
MIROC-ESM-CHEM (2.815° × 2.815°)	✓				
HadGEM2-ES (1.875° × 1.25°)	✓				
HadGEM2-A (1.25° × 1.875°)			✓	✓	✓
MRI-CGCM3 (1.125° × 1.125°)	✓		✓	✓	✓
CCSM4 (1.25° × 0.9°)	✓	✓			
NorESM1-M (2.5° × 1.875°)	✓	✓	✓	✓	✓
GFDL-CM3 (2.5° × 2.0°)	✓	✓	✓	✓	✓
GFDL-ESM 2M (2.5° × 2.0°)	✓				
CESM1-CAM5 (1.25° × 0.9°)	✓	✓			

Note. The horizontal resolutions of the models are shown in the parentheses. All the model outputs are interpolated into 1.5° × 1.5° grid. GHG = greenhouse gas.

2. Data and Methods

2.1. CMIP5 GCM Outputs

We used the daily outputs from 17 CMIP5 models (Table 1). The details of CMIP5 models and simulations are available from the website http://cmip-pcmdi.llnl.gov/cmip5/. The historical simulations with GHG-only forcing (*historical GHG*) from 15 models and aerosol-only forcing (*historical AEROSOL*) from 7 models were used to calculate the responses of PE to GHG and aerosol forcings, respectively. Some other models such as Goddard Institute for Space Studies (GISS) model have conducted the aerosol-only forcing simulation, but no daily data are available at the CMIP5 website, which are not used in his study.

2.2. PEs Definitions

We first adopted two PE indices, that is, the monthly maximum 1-day precipitation (RX1day) and the monthly maximum consecutive 5-day precipitation (RX5day), following the recommendation of the Expert Team for Climate Change Detection and Indices (X. Zhang et al., 2011). The 12 monthly PE indices were first calculated using daily data (365 data points) for each year and then the 120 values were averaged for each decade from 1866 to 2005 (i.e., 1866–1875 and 1876–1885) to suppress interannual variability that is less relevant to the long-term trend analysis.

In order to test the robustness of the results to a spectrum of PE metrics, we also defined PE based on the relative threshold at each grid box, such as the days exceeding various percentiles (90%, 95%, …, 99.9%). This was done for each decade of daily data. For example, the 99.9% PE was calculated from the three heaviest rainfall days out of the 3650 days in a decade.

2.3. Calculation of the PE Sensitivity

Previous studies have shown that PE behaved linearly with GMST (Kharin et al., 2013; Lin et al., 2016; O'Gorman & Schneider, 2009a). For example, in the Figure 1 of Lin et al. (2016), the correlation coefficient for the linear regression of the decadal averaged PE and GMST amounts to be larger than 0.8. Therefore, the sensitivity of PE changes to a given forcing ($\Delta PE/\Delta GMST$) was calculated using the linear regression method as in Lin et al. (2016). We calculated the decadal average of surface temperature, precipitation, and PE in each decade since 1866 and used the 1986–2005 as the reference period to obtain the relative change of PE (converting millimeters per day to percent). Then, we obtained the PE sensitivity (percent per degrees Celsius) by linearly regressing the PE changes to GMST changes during the 140-year time frame.

The changes in GMST were of opposite sign in the cases of GHGs and aerosols (positive for GHGs and negative for aerosols). Therefore, the process of normalization by historical GMST perturbation resulted in a signal

that was in the same direction as the actual effect in the case of GHGs, but in the opposite direction as the actual effect in the case of aerosols. However, there are several advantages to using the normalization of GMST perturbation. First, one could more intuitively state the mechanism for the different PE sensitivity to GHGs and aerosols. Second, the normalized results were a representative of the effect of future reduced aerosol emissions in the aerosol case, which was one thing highlighted in this study.

2.4. Aerosol-Cloud-Precipitation Treatment in the Model

Out of the seven models that performed the historical aerosol-only simulation with archived daily data, six models considered aerosol indirect effects and CCSM4 only included aerosol direct effect (Table 1). Among these six models, CanESM2 and IPSL-CM5A-LR only included the cloud albedo effect (so-called *first* indirect effect), and the other four models (CSIRO-Mk3-6-0, NorESM1-M, GFDL-CM3, and CESM1-CAM5) included both cloud albedo and cloud lifetime effects (so-called *second* indirect effect). See Wang (2015) and Salzmann (2016) for the details of the treatments of aerosol-cloud effects in different GCMs. The contrast of these two groups of models provides an opportunity to examine the importance of cloud lifetime effect (that is, through altering precipitation process explicitly in the model) on determining PE sensitivity to aerosol forcing.

2.5. Fast and Slow Responses to Forcings

Climate response to a given forcing can be decomposed into the fast and slow responses, corresponding to different time scales (Andrews et al., 2010). The 30-year control simulation (sstClim), aerosol perturbation simulation (sstClimAerosol), and quadrupling CO_2 perturbation simulations (sstClim4×CO_2) with fixed sea surface temperature (SST) from nine CMIP5 models were used (Table 1). The annual cycle of climatological SSTs and sea ice derived from each model's preindustrial control run was imposed and both aerosols and CO_2 were set to preindustrial levels in the sstClim simulation. The setups in sstClimAerosol and sstClim4×CO_2 were the same as in sstClim, but a forcing is imposed with aerosols specified at the year 2000 levels and a quadrupled preindustrial level of CO_2, respectively.

To get the fast component of PE sensitivity to aerosol forcing, the PE differences between sstClimAerosol and sstClim simulations were normalized by the temperature change due to year 2000 aerosol forcing (derived from fully coupled historical AEROSOL simulation). The slow component was derived by subtracting the fast component from the total response in the fully coupled historical AEROSOL simulation.

To get the fast response due to GHGs in a similar way, we need to make a correction related to the CMIP5 experiment designs. For the twentieth century fully coupled simulation, historical GHG using the forcings of CO_2 and other long-lived GHGs is available, while for the fixed-SST atmospheric-only simulation, 4×CO_2 (sstClim4×CO_2) is available. The radiative forcing from the model runs with 4×CO_2 level is 7.21 W/m^2 (Andrews et al., 2012) and the year 2000 GHG forcing is 2.5 W/m^2 (Myhre et al., 2013). Therefore, we scaled the change in PE induced by 4×CO_2 forcing by a factor of 0.35 to get the fast GHG response. The scaling factor of 0.35 was similarly adopted in previous studies (e.g., Hansen et al., 2005; Xie et al., 2013). The use of the scaling relies on the assumption that the fast precipitation response to GHGs scales linearly with radiative forcing, which is supported by previous studies (Andrews et al., 2010; Samset et al., 2016).

Note that potential biases were created by the calculation of the slow response as the residual between coupled and fixed SST simulations. The coupled simulations were historically varying, while the fixed SST simulations were repeating annual cycle. The historical mean aerosol forcing in the calculation of full PE response from the coupled simulation likely had a somewhat different proportion of absorbing to scattering aerosol relative to the year 2000 aerosol burden that was used in the fixed SST simulation (Lamarque et al., 2010). This might introduce some slight mismatches in the aerosol case. In addition, the fixed SST simulation used 4×CO_2, which must be scaled to emulate the historical GHG forcing in the coupled simulation. There were also some mismatches in the GHG case.

3. Results

3.1. Larger Sensitivity to Aerosol Forcing Across Models

Figures 1b and 1c show the sensitivity of PE to aerosol and GHG forcings based on the CMIP5 MME mean, indicating a robustly larger sensitivity of PE to aerosols than GHGs, similar to the mean precipitation result

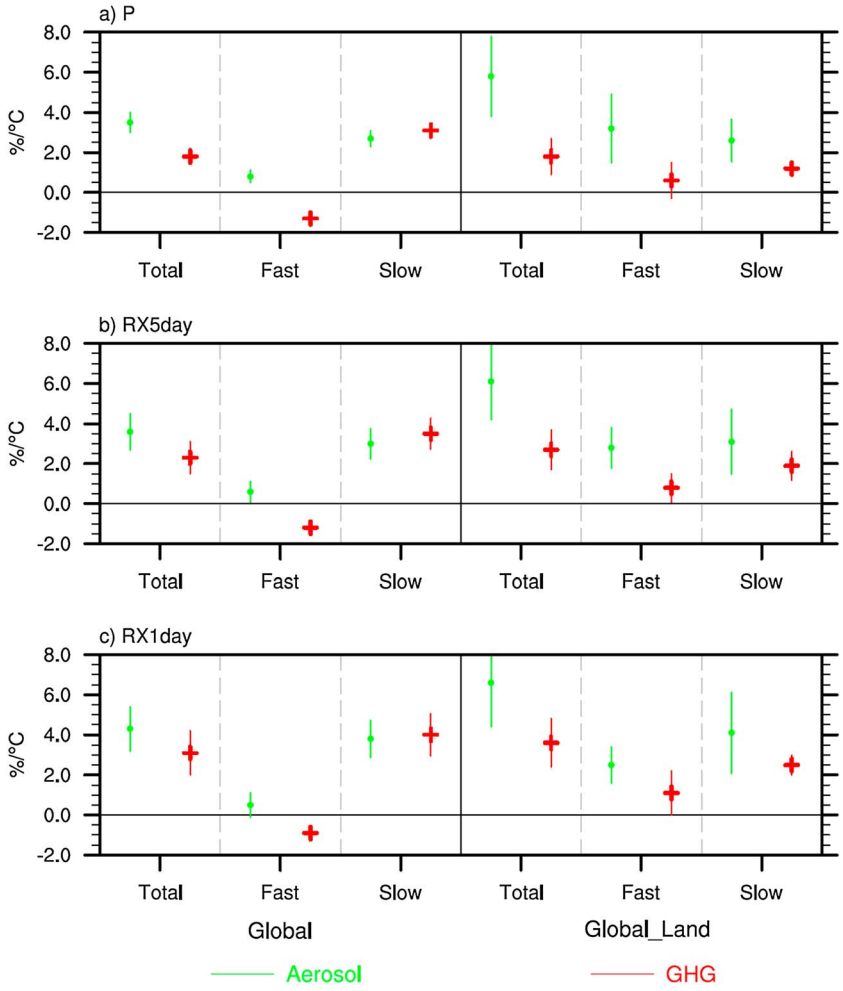

Figure 1. The Coupled Model Intercomparison Program phase 5 multi-model mean sensitivities in global- and land-mean precipitation and PEs in the total, fast and slow responses to aerosol (green) and greenhouse gas (red) forcings (units: %/°C). The error bars denote two standard deviation due to both model structure uncertainty and internal variability.

(e.g., Kvalevåg et al., 2013; Samset et al., 2016; also see Figure 1a). The aerosol/GHG-induced sensitivity ratios for globe-averaged mean precipitation, RX5day, and RX1day in the MME are 1.9, 1.6, and 1.4, respectively. The ratios for mean and extreme precipitations over land are larger than those over the globe. Over land, the corresponding ratios for mean precipitation, RX5day, and RX1day are 3.2, 2.3, and 1.8, respectively (second column in Figure 1). The specific reasons will be discussed in section 3.3.

Figure 2 shows the geographical distributions of the MME mean sensitivity in mean precipitation and PE caused by aerosols and GHGs. The spatial distributions caused by the two forcings are broadly in line with those found in Lin et al. (2016). There is a high similarity in the spatial distributions of aerosol and GHG-induced PE sensitivities. Both forcings lead to increases in mean precipitation and PE with warming over most of the globe. Notably, the PE sensitivity over most regions caused by aerosols is larger than that caused by GHGs. In particular, the aerosol forcing leads to several times greater sensitivity than GHG forcing in West Africa, eastern China, South and Southeast Asia, northwestern South America, and Eastern Europe (Figures 2f and 2i).

3.2. Fast Versus Slow Response: The Role of Atmospheric Energy Balance

The climate adjustment in the atmosphere including clouds over a shorter time scale of days to months without ocean mediation is regarded as the fast response. The climate adjustment due to the change in SST on a longer time scale of years to decades is regarded as the slow response. The decomposition of the fast and slow

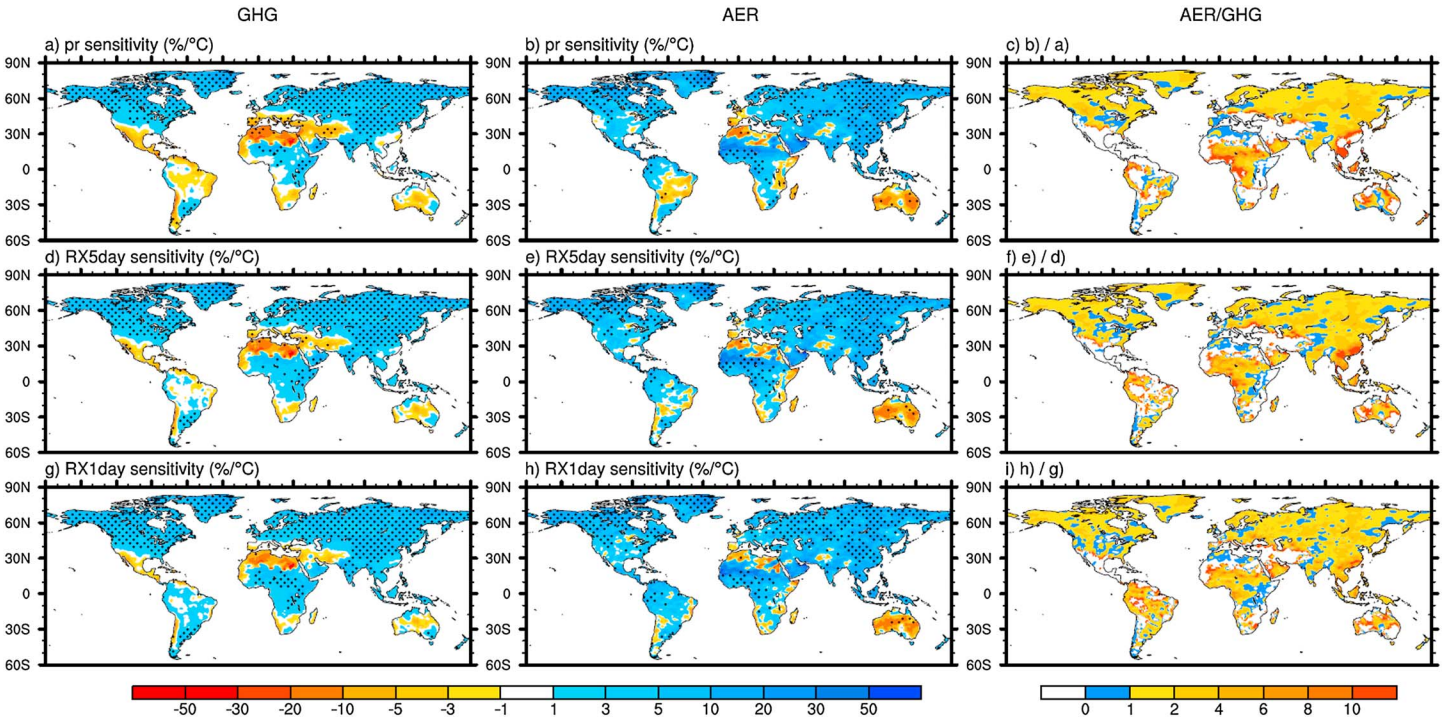

Figure 2. Geographical distributions of the Coupled Model Intercomparison Program phase 5 multimodel mean sensitivities (units: %/°C) of precipitation (pr) and precipitation extremes over land caused by greenhouse gas (GHG; a, d, and g) and aerosol (b, e, and h) forcings with the dotted regions indicating more than 80% of the models agree on the sign. The aerosol-to-GHG ratios are shown in the right column, with less-than-one regions (GHG effect stronger than aerosol) marked blue, and less-than-zero regions (opposite sign of aerosol- and GHG-caused changes) marked white.

climate responses to external forcings has been done in a few recent studies on, for example, the monsoon, Hadley circulation, and rainfall (e.g., Samset et al., 2016; Wang et al., 2017; Xu & Xie, 2015). It is the fast response that leads to the overall difference between GHG- and aerosol-induced responses for mean precipitation (Samset et al., 2016). Separation of the fast and slow PE responses, therefore, can provide useful insight. We here examine to what extent this principle holds for PE based on various definitions.

CMIP5 MME shows that the globe-averaged precipitation decreases in the fast response to GHG forcing with 1–2%/°C (Figure 1, the red in the *global fast* column), while the opposite is true for the fast response to aerosol forcing (with an increase of 0.5–1%/°C). The sign difference between the two fast responses is remarkable, which is the key reason for the different sensitivities for the mean precipitation to the two forcings, as suggested by previous studies (e.g., Kvalevåg et al., 2013; Samset et al., 2016). The slow responses due to aerosols and GHGs appear to have the same magnitude (*global slow* column in Figure 1).

The difference in the fast responses between aerosols and GHGs reflects the fact that precipitation amount is strongly constrained by atmospheric radiative cooling (Allen & Ingram, 2002), and thus, the change in precipitation is also anchored to the change in atmospheric forcing. Unlike the aerosol forcing in the twentieth century, which has a small atmospheric forcing component, atmospheric longwave heating caused by GHGs (Figure 3) suppresses the fast precipitation response to the forcing.

Does the atmospheric energy balance argument hold for PE? Figure 1 shows that the changes in globe-averaged PE (at least in the form of RX5day and RX1day) behave in a similar fashion to the mean precipitation despite a smaller difference in RX1day. Thus, this is highly suggestive that PE is also tightly constrained by the atmospheric radiative energy balance. This leads to an opposite sign of PE sensitivities in the fast responses to GHGs and aerosols, with a positive response in the aerosol case and negative response in the GHG case (global fast column in Figure 1).

Although the aerosol forcing is largely due to cooling aerosols (sulfate, nitrate, organics, etc.) that simply reflect solar radiation with little atmospheric forcing, the atmospheric heating effect of absorbing aerosols

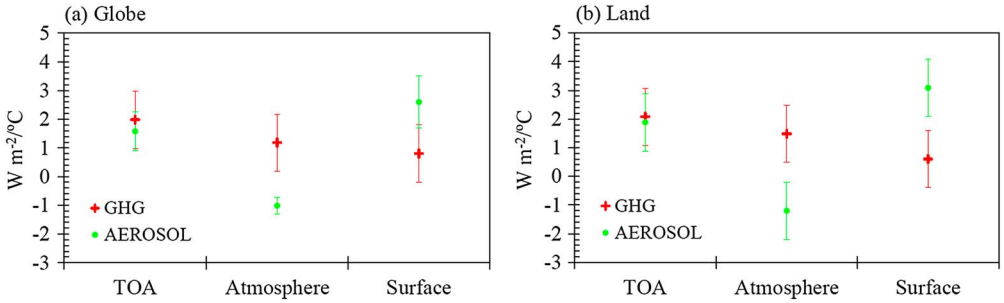

Figure 3. The Coupled Model Intercomparison Program phase 5 multimodel mean greenhouse gas (GHG) and aerosol radiative forcings at the top of the atmosphere (TOA) and surface and in the atmosphere averaged over (a) globe and (b) land when normalized by the global mean surface temperature changes (units: $W{\cdot}m^{-2}{\cdot}°C^{-1}$). The error bars denote one standard deviation due to model difference. Radiative forcing is derived from the fixed sea surface temperature simulations.

during the twentieth century should not be ignored. When normalized by a negative GMST change, total aerosol forcing that includes absorbing aerosols leads to a significant radiative cooling in the atmosphere (Figure 3), which is a representative of the effect of future reduced aerosol emissions, and thus tends to enhance the precipitation per atmospheric energy balance argument. This contrasts to the suppression effect of GHGs and explains the sign difference in the fast responses. Note that the values in Figure 1 (%/°C) and Figure 3 ($W{\cdot}m^{-2}{\cdot}°C^{-1}$) are normalized by the GMST change, so that the GHG and aerosol forcings are deemed positive at the TOA and surface. When interpreted with the actual aerosol-induced GMST changes, the atmospheric forcing due to aerosols (mainly contributed by absorbing aerosols) is positive, thus exerting a suppression effect on precipitation, which works in conjunction with the surface cooling due to total aerosols and contributes to the overall higher sensitivity (%/°C).

We also note that the atmospheric heating is completely missing when the forcing is imposed at the TOA only by perturbing solar constant (e.g., Sillmann et al., 2017). Therefore, the PE sensitivity difference between solar and GHG forcings is expected to be smaller than the aerosol and GHG difference examined here. We conclude that just like the mean precipitation, the fast responses of PE are the primary contributor to the sensitivity difference between aerosol and GHG forcings, while the slow components are of comparable scale.

3.3. Responses Over Land Versus Ocean: The Role of Dynamic and Thermodynamic Adjustments

When comparing GHG and aerosol forcings, another major difference is associated with the land and ocean contrast. The aerosol forcing is predominated over land, while the GHG forcing is wide spread over globe. Here we examine the land and ocean contrast in the PE responses to provide further insight to the overall aerosol and GHG differences.

3.3.1. Slow Component

Comparing the global (left columns in Figure 1) and land (right columns in Figure 1) responses, a main feature in precipitation, RX5day, and RX1day results is that the aerosol-to-GHG ratio is larger over land than over the globe, particularly for the slow responses where the ratio is about one for the global responses. Previous studies with the fast and slow decomposition (Kvalevåg et al., 2013; Samset et al., 2016) indicated that the mean precipitation increases with warming in the slow responses. The MME results here further show that the PE also increase with warming; and more importantly, the slow component of globe-averaged PE sensitivity is of the similar magnitudes for aerosol and GHG responses (see global slow column in Figure 1). However, averaged over the land, the aerosol-induced PE sensitivity is still about 1.6 times of that due to GHGs even for the slow responses (see global-land slow column in Figure 1).

Why does the larger response to aerosols persist over land? It is known that the change in PE has a thermodynamic contribution from change in atmospheric moisture and a dynamical contribution from change in vertical velocity synthetically (Emori & Brown, 2005; O'Gorman & Schneider, 2009a, 2009b). In other words, larger increases in atmospheric moisture and vertical ascent motion likely will lead to a larger increase in PE. Table 2 shows that for the slow responses over land when normalized by the GMST changes, the aerosol forcing leads to a slightly larger increase in column atmospheric moisture (14.8 vs. 12.7 $g{\cdot}m^{-2}{\cdot}°C^{-1}$) and a significantly smaller descending motion increase (38.9 vs. 60.9 $Pa{\cdot}day^{-1}{\cdot}°C^{-1}$) than GHG forcing. Both the dynamic and thermodynamic factors contribute to a larger PE sensitivity to aerosols in the slow response

Table 2
The CMIP5 Multimodel Mean Sensitivities in Global-/Land-Mean Vertically Integrated Atmospheric Moisture (Unit: g·m^{-2}·℃$^{-1}$) and Vertical Velocity at 500 hPa (Negative Value Indicates Ascending Motion, Unit: Pa·day^{-1}·℃$^{-1}$) in the Total, Fast, and Slow Responses to Aerosol and GHG Forcings

	Atmospheric moisture (g·m^{-2}·℃$^{-1}$)			Vertical velocity (Pa·day^{-1}·℃$^{-1}$)		
	Total	Fast	Slow	Total	Fast	Slow
GHG	14.2/14.8	0.9/2.2	13.2/12.7	−0.4/6.9	−0.2/−54.0	−0.2/60.9
AEROSOL	13.9/15.5	−0.2/0.7	14.1/14.8	−0.5/ -6.6	−0.2/−45.4	−0.3/38.9

Note. GHG = greenhouse gas.

over land. Note that the aerosol-induced changes in Table 2 are normalized by the negative GMST change. The actual aerosol forcing leads to a decrease in atmospheric moisture and an increase in vertical ascent motion in the slow response over land.

Previous studies indicated that aerosol forcing could yield large effects on land precipitation during monsoon seasons via dynamic responses (e.g., Bollasina & Ramaswamy, 2011; Polson et al., 2014; Wang et al., 2017; L. Zhang & Li, 2016). Geographically, Figure 2 shows that the larger aerosol-to-GHG ratios of the PE sensitivities over land primarily appear in the tropical and subtropical monsoon regions, such as East and Southeast Asia, Australia, West Africa, and northern South America. This implies the importance of dynamic adjustment in contributing to the larger PE sensitivity to aerosols in the total response over land, as also indicated in Table 2.

3.3.2. Fast Component

A second feature deserving attention in comparing land with global responses is that the GHG forcing results in a weak positive PE sensitivity in the fast response over land (see global-land fast column in Figure 1). This contrasts to the negative PE fast sensitivity over the globe due to GHGs (global fast column in Figure 1). The positive GHG response in the land-mean fast component is mainly because the GHG forcing boosts vertical ascending motions over land (−54.0·Pa·day^{-1}·℃$^{-1}$; Table 2). This stronger dynamical adjustment overwhelms the smaller responses in moisture content (2.2 g m^{-2}/℃).

However, the PE sensitivity caused by aerosols is still markedly larger than that caused by GHGs for the fast responses over land (global-land fast column in Figure 1). The aerosol-to-GHG ratios of sensitivities are 3.2, 2.5, and 2.3 for the fast component of precipitation, RX5day, and RX1day over land, respectively. As shown in Table 2, the GHG forcing leads to larger sensitivities of land-mean moisture content and vertical instability in the fast response. Therefore, the larger PE sensitivity to aerosols over land likely remains due to the role of atmospheric energy balance (Figure 3b) as mentioned in section 3.2, rather than the contributions of dynamic and thermodynamic adjustments.

In brief, both the global-mean dynamic and thermodynamic adjustments in the total responses to the two forcings are comparable when normalized by the GMST changes, so the contributions of them to the increase in PE are comparable on a global scale. The impacts of thermodynamic adjustments on PE in the total responses to aerosols and GHGs are comparable over land. However, there is an opposite sign of dynamic adjustments over land in the total responses to both forcings, which leads to a positive impact on PE in the aerosol case and negative impact on PE in the GHG case. Therefore, the difference of dynamic adjustment is responsible for the larger sensitivity of PE over land to aerosols relative to GHGs.

3.4. Response in Convective Versus Large-Scale Rainfall: The Role of Vertical Forcing

The different vertical structure of aerosol and GHG forcing (i.e., the opposite signs for aerosols in the atmospheric column and at the surface vs. the same signs for GHGs) (Wang, Zhang, & Zhang, 2016) may lead to the difference between PE sensitivities due to the two forcings. To be more specific, the historical aerosol emissions lead to a positive forcing in the atmosphere (due to absorbing aerosols) and negative forcing at the surface. Normalizing the historical aerosol forcing by its historical negative GMST perturbation presents an analog for the conditions that could be created by future removal of aerosol emissions. When normalized by the GMST change, the vertical structure of aerosol forcing with a negative forcing in the atmosphere (just like the effect of the removal of absorbing aerosols and their associated positive atmospheric forcing) and positive forcing at the surface is more conducive to boosting the vertical instability. This case primarily occurs over land (a negative value in the AEROSOL row of Table 2 for the total over land). On the other hand, the

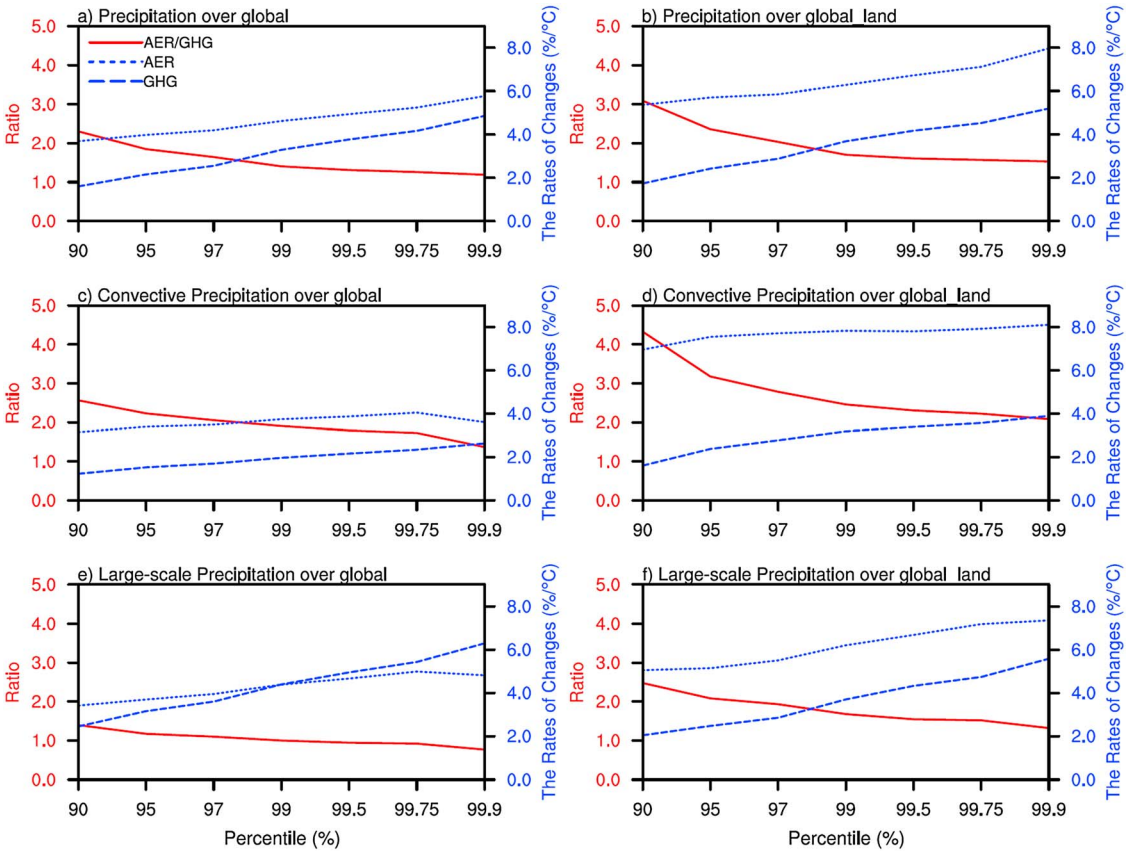

Figure 4. (a) Relative rate of changes in the precipitation extreme sensitivity (%/C) caused by aerosols (blue dotted line) and greenhouse gases (GHGs; blue dashed line), averaged over globe, and the aerosol-to-GHG ratio (red line). (b) Same as (a) averaged over land. (c and d, and e and f) Same as (a) and (b), but for simulated convective and large-scale rainfalls, respectively. All values are displayed as a function of precipitation extreme metrics (*X* axis).

vertical structure of GHG forcing tends to suppress the development of convection over land (a positive value in the GHG row of Table 2 for the total over land) due to a significantly larger heating in the atmosphere than at the surface (1.48 vs. 0.6 $W{\cdot}m^{-2}{\cdot}°C^{-1}$, Figure 3). This contributes to the larger PE sensitivity to aerosols.

The arguments above are also confirmed by Figure 4, which suggests that the larger aerosol-to-GHG ratio of the PE sensitivities in the total PE is mostly attributed to the convective precipitation over land. Figures 4e and 4f indeed indicate that the difference in the PE sensitivity between aerosols and GHGs for the large-scale PE is smaller. The aerosol-to-GHG ratio for the large-scale PE is close to one over the globe (Figure 4e), but larger over land as expected (Figure 4f).

Note that one caveat here is that the change in convective precipitation is caused by the circulation-related dynamic responses to aerosol forcing, without considering microphysical effect of aerosols on convective clouds. None of the CMIP5 models here explicitly treat the aerosol effects on convection at the subgrid scale, including, for example, the so-called *invigoration effects* as suggested by Rosenfeld et al. (2008) and Li et al. (2011). Thus, the results and interpretation provided here in regard to the convective rainfall response to aerosols is worth revisiting when more state-of-art model results (CMIP6) become available in the next few years.

4. Discussion

4.1. The Dependence Upon PE Definition

Lin et al. (2016) indicated that the aerosol-to-GHG ratios of the PE sensitivities are larger for the more loosely defined extreme precipitation indices (such as RX5day) as opposed to the more extreme indices (e.g., RX1day or RX1day_Annual as in Pendergrass et al., 2015). Previous studies argued that extreme precipitation

Table 3
The CMIP5 Multimodel Mean Precipitation Extremes Sensitivities in the Land- and Globe-Mean, Caused by Aerosol Forcing From Models With Cloud Albedo Effect Only, and Both Albedo and Lifetime Effects, Respectively (Units: %/°C)

	Global land		Globe	
	Cloud albedo	Cloud albedo and cloud lifetime	Cloud albedo	Cloud albedo and cloud lifetime
P	5.2 ± 2.2	5.7 ± 2.4	3.2 ± 0.8	3.6 ± 0.3
RX5day	5.1 ± 2.6	6.0 ± 1.4	3.0 ± 1.3	3.8 ± 0.6
RX1day	5.1 ± 2.9	6.6 ± 1.4	3.4 ± 1.6	4.4 ± 0.6

Note. The values after ± are one standard deviation due to model difference and internal variability.

persisting for a few days (i.e., more loosely defined extreme) were more related to flooding than a single-day event (Sillmann, Kharin, et al., 2013). Figure 4 further tests this dependence upon PE definition by showing the aerosol and GHG sensitivity (dotted and dashed blue lines, right *Y* axis) and their ratio (red line, left *Y* axis) over a spectrum of extreme definitions. The aerosol-to-GHG ratio is obviously larger for the *loosely* defined extremes and it gradually converges to 1 for the defined extremes that are more severe. This explains the finding by Pendergrass et al. (2015) who used the RX1day_Annual (effectively 99.7% = 1/365) as the extreme metric for which the PE sensitivity difference was indistinguishable among various forcing scenarios with different aerosol and GHG forcing composition. Sillmann et al. (2017) also reported that changes in PE (expressed as annual maximum 1-day precipitation) did not seem to depend on the forcing mechanism when comparing CO_2 with solar forcing.

4.2. The Dependence Upon Aerosol Schemes in GCMs

One unique feature of aerosols is that they can alter the cloud and precipitation processes by changing the cloud particle number concentration and cloud particle sizes, which affects the cloud albedo (Twomey, 1977) and cloud lifetime (Albrecht, 1989). Lin et al. (2016) hinted that the enhancement of large-scale stratus cloud lifetime by suppressing precipitation may explain the larger PE sensitivities to aerosols, but they did not provide quantitative analyses. Here we divide the CMIP5 GCMs used in this study into two groups (method in section 2.4) to examine the importance of aerosol cloud lifetime effect on determining PE sensitivity. Group 1 (two models) only includes cloud albedo effect, and Group 2 (four models) includes both cloud albedo and cloud lifetime effects.

Table 3 shows that the aerosol-induced PE sensitivity seems larger in models with both cloud effects than those with only cloud albedo effect. This is true for both globe-averaged and land-averaged results. However, a challenge to distinguishing the role of cloud lifetime effect is the limited number of available models. Only six models performed the historical aerosol-only simulation. Among them, two include the cloud albedo effect and four include both cloud effects. Furthermore, the structural uncertainties between CMIP5 models go beyond the treatment of aerosol-cloud interactions, which, for example, include convective schemes among others, although we find no systematic differences between these two groups other than that Group 2 explicitly treats cloud lifetime effect. Therefore, it is not clear from the present analysis that the stronger PE sensitivity to aerosols can be entirely attributed to the explicit treatment of cloud lifetime effect. The role of the different aerosol-cloud processes should be acknowledged, but this appears not to be possible within the presently available dataset. It is our future research effort to revisit this issue by running the same GCMs with and without the treatment of cloud life time effect.

It should also be noted that the CMIP5 models only treat the microphysical effect of aerosols on the large-scale clouds and precipitation, but not on the convective clouds and precipitation. However, our results show that the aerosol and GHG differences in the large-scale PE sensitivities (Figures 4e and 4f) are smaller. These imply that the microphysical effects of aerosols via the large-scale cloud and rainfall processes might not be the primary cause of the stronger PE sensitivity to aerosol forcing.

5. Summary

Using the twentieth century historical MME simulations from the CMIP5, we examine the difference in the PE sensitivity to aerosol and GHG forcings. Then, the physical mechanisms responsible for the different PE sensitivities due to the two forcings are analyzed. The CMIP5 MME simulations robustly show a larger sensitivity of PE to aerosols than GHGs, especially over land, supporting the conclusions based on a single GCM (Lin et al., 2016). The aerosol/GHG-induced sensitivity ratios for globe-averaged mean precipitation, RX5day, and RX1day in the MME are 1.9, 1.6, and 1.4, respectively. The ratios for mean and extreme precipitations over land are larger than those over the globe. Over land, the corresponding ratios for mean precipitation, RX5day, and RX1day are 3.2, 2.3, and 1.8, respectively. In particular, the aerosol forcing leads to several times greater

sensitivity than GHG forcing in West Africa, eastern China, South and Southeast Asia, northwestern South America, and Eastern Europe.

The atmospheric energy balance, dynamic adjustment, and vertical structure of forcing, all contribute to the difference in the PE sensitivity to aerosol and GHG forcings. It is shown that the fast response is the primary cause of the difference in the PE sensitivity between the two forcings, while the globe-mean slow components are relatively comparable, as for the mean precipitation. There is an opposite sign of globe-mean PE sensitivities in the fast responses to GHGs and aerosols, with a positive response in the aerosol case and negative response in the GHG case. The actual aerosols induce an atmospheric heating effect (mainly due to the absorbing aerosols). When normalized by a negative GMST change, the aerosols lead to a radiative cooling in the atmosphere and thus tend to enhance the PE. This implies that PE is tightly constrained by the atmospheric radiative energy balance. Moreover, there is an opposite sign of normalized dynamic adjustments to both forcings in the total responses over land (increase in convection for aerosols but decrease in convection for GHGs), which is responsible for the larger PE sensitivity over land to aerosols relative to GHGs.

Note that normalizing the historical aerosol forcing by its historical negative GMST perturbation presents an analog for the conditions that could be created by future reduced aerosol emissions. Our results indicate that when normalized by the negative GMST change, the vertical structure of aerosol forcing with a negative forcing in the atmosphere (just like the effect of the removal of absorbing aerosols and their associated positive atmospheric forcing) and positive forcing at the surface is more conducive to boosting the vertical instability over land. However, the corresponding structure of GHG forcing tends to suppress the development of convection over land due to a larger heating in the atmosphere than at the surface. This contributes to the larger PE sensitivity to aerosols. The microphysical effects of aerosol on the large-scale rainfall processes might also play a role but might not be the primary cause of the stronger PE sensitivity to aerosols than GHGs.

This study also reinforces the dependence of sensitivity difference between aerosols and GHGs on the PE definition. The aerosol-to-GHG ratio of the PE sensitivities is greater for more loosely defined PE, and it gradually converges toward the unity when the PE definition becomes more severe. We further highlight the importance of considering the changes in anthropogenic aerosol emissions and other short-lived climate forcing for projecting future change not only in mean precipitation (Shine et al., 2015) but also in PE.

Acknowledgments
This study was supported by the National Key Research and Development Program of China (2016YFA0602701 and 2016YFC0203306), the (key) National Natural Science Foundation of China (91644211, 91644225, and 41575139), Fundamental Research Funds for the Central Universities (17lgpy32), and CAMS Foundation for Development of Science and Technology (2018KJ047). We acknowledge the World Climate Research Programme's Working Group on Coupled Modeling, which is responsible for CMIP. The access to the data and technical aid is provided by the German Climate Computing Centre (DKRZ; https://esgf-data.dkrz.de/search/cmip5-dkrz/), with funding from the Federal Ministry for Education and Research.

References

Albrecht, B. A. (1989). Aerosols, cloud microphysics, and fractional cloudiness. *Science*, *245*(4923), 1227–1230. https://doi.org/10.1126/science.245.4923.1227

Allen, M. R., & Ingram, W. J. (2002). Constraints on future changes in climate and the hydrologic cycle. *Nature*, *419*(6903), 224–232. https://doi.org/10.1038/nature01092

Andrews, T., Forster, P. M., Boucher, O., Bellouin, N., & Jones, A. (2010). Precipitation, radiative forcing and global temperature change. *Geophysical Research Letters*, *37*, L14701. https://doi.org/10.1029/2010GL043991

Andrews, T., Gregory, J. M., Webb, M. J., & Taylor, K. E. (2012). Forcing, feedbacks and climate sensitivity in CMIP5 coupled atmosphere-ocean climate models. *Geophysical Research Letters*, *39*, L09712. https://doi.org/10.1029/2012GL051607

Bollasina, M. A., & Ramaswamy, V. (2011). Anthropogenic aerosols and the weakening of the south Asian summer monsoon. *Science*, *334*(6055), 502–505. https://doi.org/10.1126/science.1204994

Easterling, D. R., Meehl, G. A., Parmesan, C., Changnon, S. A., Karl, T. R., & Mearns, L. O. (2000). Climate extremes: Observations, modeling, and impacts. *Science*, *289*(5487), 2068–2074. https://doi.org/10.1126/science.289.5487.2068

Emori, S., & Brown, S. J. (2005). Dynamic and thermodynamic changes in mean and extreme precipitation under changed climate. *Geophysical Research Letters*, *32*, L17706. https://doi.org/10.1029/2005GL023272

Hansen, J., Sato, M., Ruedy, R., Nazarenko, L., Lacis, A., Schmidt, G. A., et al. (2005). Efficacy of climate forcings. *Journal of Geophysical Research*, *110*, D18104. https://doi.org/10.1029/2005JD005776

Hartman, D. L., Tank, A. M. G. K., Rusicucci, M., Alexander, L. V., Broenniman, B., Charabi, Y., et al. (2013). Observations: Atmosphere and surface. In T. F. Stocker, et al. (Eds.), *Climate change 2013: The physical science basis. Contribution of Working Group I to the Fifth Assessment Report of the Intergovernmental Panel on Climate Change* (pp. 159–254). Cambridge, U. K., and New York: Cambridge University press.

Hoesly, R. M., Smith, S. J., Feng, L., Klimont, Z., Janssens-Maenhout, G., Pitkanen, T., et al. (2018). Historical (1750–2014) anthropogenic emissions of reactive gases and aerosols from the Community Emissions Data System (CEDS). *Geoscientific Model Development*, *11*(1), 369–408. https://doi.org/10.5194/gmd-11-369-2018

Kharin, V. V., Zwiers, F. W., Zhang, X., & Wehner, M. (2013). Changes in temperature and precipitation extremes in the CMIP5 ensemble. *Climatic Change*, *119*(2), 345–357. https://doi.org/10.1007/s10584-013-0705-8

Knapp, A. K., Beier, C. B. D. D., Classen, A. T., Luo, Y., Reichstein, M., Smith, M. D., et al. (2008). Consequences of more extreme precipitation regimes for terrestrial ecosystems. *Bioscience*, *58*(9), 811–821. https://doi.org/10.1641/B580908

Kvalevåg, M. M., Samset, B. H., & Myhre, G. (2013). Hydrological sensitivity to greenhouse gases and aerosols in a global climate model. *Geophysical Research Letters*, *40*, 1432–1438. https://doi.org/10.1002/grl.50318

Lamarque, J.-F., Bond, T. C., Eyring, V., Granier, C., Heil, A., Klimont, Z., et al. (2010). Historical (1850–2000) gridded anthropogenic and biomass burning emissions of reactive gases and aerosols: Methodology and application. *Atmospheric Chemistry and Physics*, *10*(15), 7017–7039. https://doi.org/10.5194/acp-10-7017-2010

Li, C., McLinden, C., Fioletov, V., Krotkov, N., Carn, S., Joiner, J., et al. (2017). India is overtaking China as the world's largest emitter of anthropogenic sulfur dioxide. *Scientific Reports*, *7*(1), 14304. https://doi.org/10.1038/s41598-017-14639-8

Li, Z., Niu, F., Fan, J., Liu, Y., Rosenfeld, D., & Ding, Y. (2011). Long-term impacts of aerosols on the vertical development of clouds and precipitation. *Nature Geoscience*, *4*(12), 888–894. https://doi.org/10.1038/ngeo1313

Lin, L., Gettelman, A., Fu, Q., & Xu, Y. (2018). Simulated differences in 21st century aridity due to different scenarios of greenhouse gases and aerosols. *Climatic Change*, *146*(3–4), 407–422. https://doi.org/10.1007/s10584-016-1615-3

Lin, L., Wang, Z. L., Xu, Y. Y., & Fu, Q. (2016). Sensitivity of precipitation extremes to radiative forcing of greenhouse gases and aerosols. *Geophysical Research Letters*, *43*, 9860–9868. https://doi.org/10.1002/2016GL070869

Moss, R. H., Edmonds, J. A., Hibbard, K. A., Manning, M. R., Rose, S. K., van Vuuren, D. P., et al. (2010). The next generation of scenarios for climate change research and assessment. *Nature*, *463*, 747–756. https://doi.org/10.1038/nature08823

Myhre, G., Forster, P. M., Samset, B. H., Hodnebrog, Ø., Sillmann, J., Aalbergsjø, S. G., et al. (2017). PDRMIP: A Precipitation Driver and Response Model Intercomparison Project—Protocol and preliminary results. *Bulletin of the American Meteorological Society*, *98*(6), 1185–1198. https://doi.org/10.1175/BAMS-D-16-0019.1

Myhre, G., Shindell, D., Bréon, F.-M., Collins, W., Fuglestvedt, J., Huang, J., et al. (2013). Anthropogenic and natural radiative forcing. In T. F. Stocker, et al. (Eds.), *Climate change 2013: The physical science basis. Contribution of Working Group I to the Fifth Assessment Report of the Intergovernmental Panel on Climate Change*, (pp. 659–740). Cambridge, UK, New York, NY, USA: Cambridge University Press.

O'Gorman, P. A. (2015). Precipitation extremes under climate change. *Current Climate Change Reports*, *1*(2), 49–59. https://doi.org/10.1007/s40641-015-0009-3

O'Gorman, P. A., & Schneider, T. (2009a). Scaling of precipitation extremes over a wide range of climates simulated with an idealized GCM. *Journal of Climate*, *22*(21), 5676–5685. https://doi.org/10.1175/2009JCLI2701.1

O'Gorman, P. A., & Schneider, T. (2009b). The physical basis for increases in precipitation extremes in simulations of 21st-century climate change. *Proceedings of the National Academy of Sciences of the United States of America*, *106*(35), 14,773–14,777. https://doi.org/10.1073/pnas.0907610106

Pendergrass, A. G., Lehner, F., Sanderson, B. M., & Xu, Y. (2015). Does extreme precipitation intensity depend on the emissions scenario? *Geophysical Research Letters*, *42*, 8767–8774. https://doi.org/10.1002/2015GL065854

Polson, D., Bollasina, M., Hegerl, G. C., & Wilcox, L. J. (2014). Decreased monsoon precipitation in the northern hemisphere due to anthropogenic aerosols. *Geophysical Research Letters*, *41*, 6023–6029. https://doi.org/10.1002/2014GL060811

Rao, S., Klimont, Z., Smith, S. J., Dingenen, R. V., Dentener, F., Bouwman, L., et al. (2016). Future air pollution in the shared socio-economic pathways. *Global Environmental Change*, *42*, 346–358.

Rosenfeld, D., Lohmann, U., Raga, G. B., O'Dowd, C. D., Kulmala, M., Fuzzi, S., et al. (2008). Flood or drought: How do aerosols affect precipitation? *Science*, *321*(5894), 1309–1313. https://doi.org/10.1126/science.1160606

Salzmann, M. (2016). Global warming without global mean precipitation increase? *Science Advances*, *2*(6), e1501572. https://doi.org/10.1126/sciadv.1501572

Samset, B. H., Myhre, G., Forster, P. M., Hodnebrog, Ø., Andrews, T., Faluvegi, G., et al. (2016). Fast and slow precipitation responses to individual climate forcers: A PDRMIP multimodel study. *Geophysical Research Letters*, *43*, 2782–2791. https://doi.org/10.1002/2016GL068064

Shine, K. P., Allan, R. P., Collins, W. J., & Fuglestvedt, J. S. (2015). Metrics for linking emissions of gases and aerosols to global precipitation changes. *Earth System Dynamics*, *6*(2), 525–540. https://doi.org/10.5194/esd-6-525-2015

Sillmann, J., Kharin, V. V., Zwiers, F. W., Zhang, X., & Bronaugh, D. (2013). Climate extremes indices in the CMIP5 multimodel ensemble: Part 2. Future climate projections. *Journal of Geophysical Research: Atmospheres*, *118*, 2473–2493. https://doi.org/10.1002/jgrd.50188

Sillmann, J., Pozzoli, L., Vignati, E., Kloster, S., & Feichter, J. (2013). Aerosol effect on climate extremes in Europe under different future scenarios. *Geophysical Research Letters*, *40*, 2290–2295. https://doi.org/10.1002/grl.50459

Sillmann, J., Stjern, C. W., Myhre, G., & Forster, P. M. (2017). Slow and fast response of mean and extreme precipitation to different forcing in CMIP5 simulations. *Geophysical Research Letters*, *44*, 6383–6390. https://doi.org/10.1002/2017GL073229

Twomey, S. (1977). The influence of pollution on the shortwave albedo of clouds. *Journal of the Atmospheric Sciences*, *34*(7), 1149–1152. https://doi.org/10.1175/1520-0469(1977)034<1149:TIOPOT>2.0.CO;2

Wang, C. (2015). Anthropogenic aerosols and the distribution of past large-scale precipitation change. *Geophysical Research Letters*, *42*, 10,876–10,884. https://doi.org/10.1002/2015GL066416

Wang, Z. L., Lin, L., Yang, M., & Xu, Y. (2016). The effect of future reduction in aerosol emissions on climate extremes in China. *Climate Dynamics*, *47*(9-10), 2885–2899. https://doi.org/10.1007/s00382-016-3003-0

Wang, Z. L., Lin, L., Yang, M., & Xu, Y.,& Li, J. (2017). Disentangling fast and slow responses of the East Asian summer monsoon to reflecting and absorbing aerosol forcings. *Atmospheric Chemistry and Physics*, *17*(18), 11,075–11,088. https://doi.org/10.5194/acp-17-11075-2017

Wang, Z. L., Zhang, H., & Zhang, X. Y. (2016). Projected response of East Asian summer monsoon system to future reductions in emissions of anthropogenic aerosols and their precursors. *Climate Dynamics*, *47*(5-6), 1455–1468. https://doi.org/10.1007/s00382-015-2912-7

Westra, S., Alexander, L. V., & Zwiers, F. W. (2013). Global increasing trends in annual maximum daily precipitation. *Journal of Climate*, *26*(11), 3904–3918. https://doi.org/10.1175/JCLI-D-12-00502.1

Xie, S. P., Lu, B., & Xiang, B. (2013). Similar spatial patterns of climate responses to aerosol and greenhouse gas changes. *Nature Geoscience*, *6*(10), 828–832. https://doi.org/10.1038/ngeo1931

Xu, Y., Lamarque, J. F., & Sanderson, B. M. (2015). The importance of aerosol scenarios in projections of future heat extremes. *Climatic Change*, *146*(3-4), 393–406. https://doi.org/10.1007/s10584-015-1565-1

Xu, Y., & Xie, S. P. (2015). Ocean mediation of tropospheric response to reflecting and absorbing aerosols. *Atmospheric Chemistry and Physics*, *15*(10), 5827–5833. https://doi.org/10.5194/acp-15-5827-2015

Zhang, L., & Li, T. (2016). Relative roles of anthropogenic aerosols and greenhouse gases in land and oceanic monsoon changes during past 156 years in CMIP5 models. *Geophysical Research Letters*, *43*, 5295–5301. https://doi.org/10.1002/2016GL069282

Zhang, X., Alexander, L., Hegerl, G. C., Jones, P., Tank, A. K., Peterson, T. C., et al. (2011). Indices for monitoring changes in extremes based on daily temperature and precipitation data. *Wiley Interdisciplinary Reviews: Climate Change*, *2*(6), 851–870. https://doi.org/10.1002/wcc.147